

Artificial neural networks for simulating wind effects on sprinkler distribution patterns

H. Sayyadi¹*, A. A. Sadraddini¹, D. Farsadi Zadeh¹ and J. Montero²

¹ Department of Water Engineering, Agricultural Faculty, University of Tabriz, Tabriz, Iran

² Centro Regional de Estudios del Agua, Universidad de Castilla-La Mancha, Campus Universitario, sn, 02071, Albacete, Spain

Abstract

A new approach based on Artificial Neural Networks (ANNs) is presented to simulate the effects of wind on the distribution pattern of a single sprinkler under a center pivot or block irrigation system. Field experiments were performed under various wind conditions (speed and direction). An experimental data from different distribution patterns using a Nelson R3000 Rotator[®] sprinkler have been split into three and used for model training, validation and testing. Parameters affecting the distribution pattern were defined. To find an optimal structure, various networks with different architectures have been trained using an Early Stopping method. The selected structure produced $R^2 = 0.929$ and $RMSE = 6.69$ mL for the test subset, consisting of a Multi-Layer Perceptron (MLP) neural network with a backpropagation training algorithm; two hidden layers (twenty neurons in the first hidden layer and six neurons in the second hidden layer) and a tangent-sigmoid transfer function. This optimal network was implemented in MATLAB[®] to develop a model termed ISSP (Intelligent Simulator of Sprinkler Pattern). ISSP uses wind speed and direction as input variables and is able to simulate the distorted distribution pattern from a R3000 Rotator[®] sprinkler with reasonable accuracy ($R^2 > 0.935$). Results of model evaluation confirm the accuracy and robustness of ANNs for simulation of a single sprinkler distribution pattern under real field conditions.

Additional key words: backpropagation; distortion by wind; ISSP; MLP neural networks; simulation; sprinkler; water application.

Resumen

Redes neuronales artificiales para simular el efecto del viento sobre el patrón de distribución del agua de un aspersor

Se presenta un nuevo modelo basado en la técnica de Redes Neuronales Artificiales (RNA) para simular el efecto del viento sobre la distribución de agua de un aspersor, en un sistema estacionario o en equipos pivote. Se han realizado una serie de ensayos experimentales con diferentes velocidades y direcciones de viento, para el emisor Rotator R3000 de Nelson. El conjunto de datos obtenidos para los diferentes patrones de distribución del agua han sido divididos en tres grupos, y utilizados en las correspondientes fases de entrenamiento, análisis y validación. Se han definido los parámetros que influyen sobre el patrón de distribución de agua. Con el fin de encontrar una estructura de red óptima, varias redes con diferente arquitectura han sido entrenadas usando un método supervisado. Con la estructura óptima se consiguió un $R^2 = 0,929$ y $RMSE = 6,69$ mL para el grupo de ensayos correspondientes a la red *Multi-Layer Perceptron (MLP)* mediante el algoritmo de aprendizaje supervisado con retroalimentación, dos niveles de capas ocultas (veinte neuronas en el primer nivel y seis neuronas en el segundo) y una función de transferencia tangente hiperbólica. Esta red optimizada fue implementada en MATLAB para desarrollar un modelo llamado ISSP (Simulador Inteligente del Modelo de Distribución). ISSP utiliza la velocidad y dirección de viento como variables de entrada y tiene la capacidad de simular el modelo distorsionado de la distribución de agua de un emisor Rotator R3000 con una buena precisión ($R^2 > 0,935$). Los resultados confirman la precisión y robustez de las técnicas de RNA para simular el patrón de distribución del agua de un aspersor en condiciones de campo.

Palabras clave adicionales: aplicación de agua; aspersión; distorsión por el viento; ISSP; redes neuronales MLP; retroalimentación; simulación.

*Corresponding author: habib.sayyadi@gmail.com

Received: 06-09-11. Accepted: 28-09-12

Abbreviations used: ANNs (artificial neural networks); ISSP (intelligent simulator of sprinkler pattern); MLP (multi-layer perceptron); NRMSE (normalized root mean square error); PR (precipitation rate); RMSE (root mean square error).

Introduction

The water distribution pattern and spacing of sprinklers are two important factors that can affect the application uniformity of sprinkler irrigation systems. For a particular sprinkler with a given nozzle size that works under an optimal operating pressure in field conditions, the resulting water distribution depends on wind speed. Wind causes the distortion of the distribution pattern, and this increases with increasing wind speed (Keller & Bliesner, 1990).

To avoid laborious field tests and to improve the design of irrigation systems, several studies have been conducted over the last 30 years to develop irrigation simulation models which can be used for the estimation of water distribution patterns of irrigation systems under real or controlled conditions. These models have been categorized to ballistic, semi-empirical and statistical (Granier *et al.*, 2003).

The most common approach of sprinkler irrigation modeling is the ballistic method that is based on simulating trajectory of individual drops. A sprinkler is considered as a device emitting water drops in different diameters from a nozzle, which travel separately until landing on the soil surface (or crop canopy, or experimental catch-can). For a given sprinkler configuration in a no-wind condition, droplet diameter is a major factor that affects the travel distances of droplets (*i.e.* the horizontal distance between droplet landing point and the sprinkler nozzle). The flight path of each droplet is subjected to an initial velocity vector and a wind vector (parallel to the ground surface) which can be determined using ballistic theory. Gravity and drag are two other forces that act on each water droplet in vertical and opposite of drop trajectory directions, respectively. Regarding the ground, the droplet velocity is equal to the velocity of the drop in the air plus the wind vector (Playan *et al.*, 2006). The major advance of ballistic models has occurred in the last few decades and several irrigation simulation models have been developed (Fukui *et al.*, 1980; Vories *et al.*, 1987; Seginer *et al.*, 1991a; Carrion *et al.*, 2001; Montero *et al.*, 2001; Dechmi *et al.*, 2004; Lorenzini, 2004; De Wrachien & Lorenzini, 2006; Playan *et al.*, 2006; Yan *et al.*, 2010).

Simulating the modified shape of distribution patterns in accordance with initial shape of wetted area and wind conditions (speed and direction) is the basis for semi-empirical methods. It is assumed that the distribution pattern of water applied from a single sprinkler has a flexible shape on the soil surface. The

shape of distribution pattern in no-wind condition depends only on sprinkler configuration and operating pressure and could be derived from radial distributions of water measured with laboratory tests. Wind distorts this shape and the objective of semi-empirical models is to find a relationship between observed distortion and wind conditions. Calibration of such models is typically carried out using spatial distribution patterns measured in field conditions (Granier *et al.*, 2003). Seginer *et al.* (1991b) used water distribution patterns measured in different wind speeds to produce interpolated maps that take into consideration evaporation and drift losses. Han *et al.* (1994) assumed an ellipse as the base shape of a pattern and developed a simulation model that uses shape functions to estimate modified water distributions across four principal sections of the pattern. Richards & Weatherhead (1993), for simulating wind-distorted distribution pattern using a measured no-wind pattern, developed an empirical model that uses a complex series of algorithms and six empirical parameters. Based on semi-empirical considerations and using a combination of beta functions, Le Gat & Molle (2000) and Molle & Le Gat (2000) developed a model to simulate the application pattern of a single rotating sprinkler, and to describe its performance in both windy and no-wind conditions.

The statistical approach could be applied to a set of sprinklers: line or complete solid set cover (Karmeli, 1978), center pivot (Heerman *et al.*, 1992), or to a single sprinkler (Solomon & Bezdek, 1980). By defining a limited number of parameters, observed water distribution curves or maps under an isolated sprinkler in various operating conditions have been adjusted to laws of probabilistic distribution (Solomon & Bezdek, 1980). The adjustment could be performed using several simultaneous measurement series according to statistical criterion (Le Gat & Molle, 2000). The radial distribution curve from the sprinkler is identified and then the spatial distribution pattern in the wetted area can be estimated by generalizing it.

Artificial Neural Networks (ANNs) are an emerging, computational or mathematical tool that has been implemented for modeling a wide range of complex and multivariate real-world systems. These networks that mimic characteristics of the biological neural systems have some remarkable advantages such as nonlinearity, high parallelism, robustness, fault and failure tolerance, learning ability, handling imprecise and fuzzy information, and generalization capability. Without any assumption and knowledge about the underlying prin-

principles, ANNs are able to precisely extract the generalized relationship between input and output data and their accuracy increases with increasing of available data (Basheer & Hajmeer, 2000; Jain *et al.*, 2004).

An important aspect of ANNs is multi-layer feed-forward networks. In general, this class of network consists of multiple interconnected layers which are: an input layer that contains a set of sensory units (source nodes), one or more hidden layers of computation nodes, and an output layer. The input signal propagates layer-by-layer through the network only in a forward direction. These neural networks are commonly referred to as a Multi-Layer Perceptron (MLP).

In recent decades, the application of ANNs in field water engineering has increased. This approach has been used for understanding the relationships between rainfall-runoff processes (Hsu *et al.*, 1995; Fernando & Jayawardana, 1998; Shresta *et al.*, 2005), evapotranspiration modeling (Khoob, 2007; Ozkan *et al.*, 2011), estimation of suspended sediments (Ciğizoğlu, 2002), modeling of water quality parameters (Schleiter *et al.*, 1999; Karul *et al.*, 2000; Maier & Dandy, 2000), studies of flow-pollutions in soil (Yang *et al.*, 1997; Schmitz *et al.*, 2002; Jain *et al.*, 2004), and predicting water distributions under trickle irrigation (Lazarovitch *et al.*, 2009; Hinnel *et al.*, 2010).

The aim of this paper is to develop and evaluate a new approach based on MLP neural networks to simulate the wind distorted water distribution patterns under field conditions. Such a model has various advantages, including 1) the simplicity of model development for any sprinkler via completing 5-6 experimental tests at differing wind speeds; 2) ANN based models unlike ballistic models do not require numerical or analytical procedures for solving dynamic equations of droplet ballistics and determining droplet sizes; and 3) in the proposed model, the distribution pattern is generated through a point-by-point calculation of water amount and the model has ability to estimate water amount at each point in the ground with a relatively good accuracy.

Material and methods

Field experiments

Experimental tests have been conducted for various wind speeds and directions at the Research Centre of Agricultural Faculty, University of Tabriz, Iran, to obtain water distribution patterns for the sprinkler. All

conditions for the experiments, including catch-can spacing, catch-can shape and size, test duration and recording of climatic data were implemented in accordance with ISO 8026 (ISO, 1995) and ASAE S398.1 (ASAE, 1985) standards.

The Nelson R3000 Rotator[®] sprinkler operates with a proven, patented drive principle and simplicity of design with only one moving part. This sprinkler, with throw distance of 15.2-22.6 m and operating pressure range of 100-340 kPa (15-50 psi) is classified as a low pressure sprinkler. The expected Christiansen uniformity coefficient (CU) for the R3000 Rotator[®] is above 95% at various operational conditions (Kincaid, 2005). A CU of below 70% is not acceptable in sprinkler irrigation (Keller & Bliesner, 1990).

The R3000 Rotator[®] can be equipped with various plates for different applications (Anonymous, 2008). The red plate utilizing 6 streams was used in this study; the sprinkler was equipped with a 4.76 mm nozzle. The operating pressure of sprinkler was fixed at 140 kPa (20 psi) using a pressure regulator. Nozzle flow rate under these conditions was approximately 0.28 L s⁻¹. Each individual experiment lasted 1 with about 1 m³ of water being applied during each test.

A network of 21 × 21 catch-cans was placed at the testing stand at a spacing of 1.25 m × 1.25 m. The sprinkler was placed in the center of the network at a height of 1.80 m using a metal frame, and the point under the sprinkler position was without a catch-can, therefore in total 440 catch-cans were used in the network. Water volumes collected in the catch-cans were measured after each experiment. Fig. 1 shows schematic of the single sprinkler testing network.

Climate data and weather conditions (*e.g.* temperature, air humidity, and speed and direction of wind at the height of 2-m from ground level) were recorded on a 1-min frequency and averaged during the test using an automatic digital weather station, located 20-m away from the test site. The minimum and maximum averaged wind speeds during experimental tests were 0.63 m s⁻¹ and 6.98 m s⁻¹, respectively.

Problem definition and formulation

Appropriate definition and formulation of the problem is an important step in the development of successful ANN-based projects. In this study, it is assumed that there are some spatial distribution patterns which are measured under real field conditions for

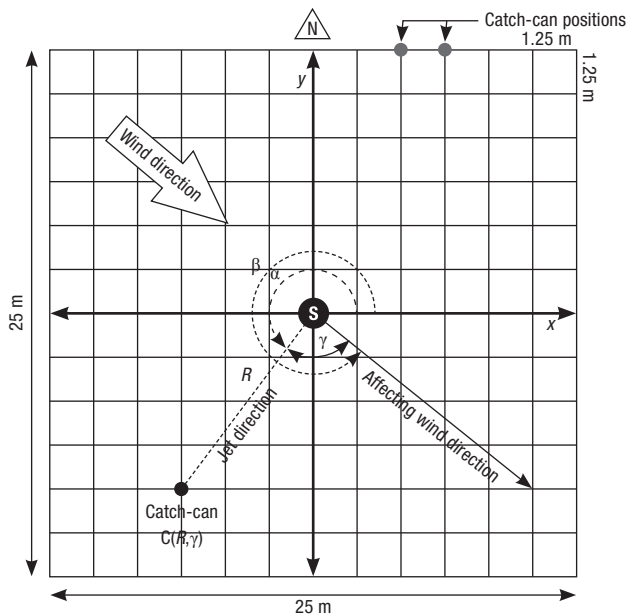


Figure 1. Schematic of testing stand and defined parameters of problem (S : sprinkler position; R : radial distance to catch-can [$C(R,\gamma)$]; α : angle of jet trajectory vector; β : angle of affecting wind vector; γ : difference between β and α).

various wind speeds, and simulating distribution patterns in none measured wind speeds is the objective of ANNs-based model. In fact, ANNs would be used here as an interpolation tool for developing a model to simulate the wind distorted distribution pattern of a sample single sprinkler. A dataset of water volumes collected in catch-cans (*i.e.* precipitation rate; PR) for each experiment were used as the targets of the neural network.

The radial distance (R) of catch-cans to the sprinkler indicates the horizontal travel distance of emitted droplets and the two alternative parameters of wind vector (*i.e.* speed, V , and its direction) were considered as the two most important parameters. A trigonometric circle has been employed to present the direction of wind and therefore an angle of zero is related to wind direction from West to East. As illustrated in Fig. 1, the incidence angle of the jet trajectory vector and wind vector is named γ that is a representative for drag forces acting on a jet element.

Each catch-can at the test network is related to a function of $C(R,\gamma)$, in which R is a constant for any given catch-can but γ varies in relation to wind direction for each individual test. Thus, volume of collected water in each catch-can for any wind speed ($PR_{C(R,\gamma),V}$) composed the output neuron of the ANN with the neurons of the input layer consisting of R , γ and V .

Design and training of networks

Fig. 2 represents a schematic of the MLP neural networks. The number of neurons in the input and output layers was set with respect to the formulation of the problem, so there were 3 and 1 neuron(s) in the input and output layers, respectively. However, determining the most appropriate number of neurons in the hidden layers is more flexible. In the present study to attain an optimal network structure, the number of neurons in the hidden layer(s) was determined by several trials.

A variety of learning algorithms could be implemented for training MLP neural networks and the most common algorithm is error backpropagation. Basically, an error backpropagation algorithm consists of a forward pass and a backward pass through the different layers of the network. In the forward pass, a set of data, as input vector are applied to the sensory nodes of the network, and therefore a set of outputs is produced as the actual response of the network. All the weights of the network are fixed during the forward pass. Then, the error signal is produced by subtracting the network responses from target values and propagated backward through the network to adjust all weights in accordance with an error-correction rule (Haykin, 1999). The backpropagation algorithm is shown in Eq. [1]:

$$\mathbf{x}_{k+1} = \mathbf{x}_k - \alpha_k \mathbf{g}_k \quad [1]$$

where \mathbf{x}_k is the vector of weights and biases at the iteration of k ; α_k is the learning rate at the iteration of k ; \mathbf{g}_k is the gradient at the iteration of k .

Various backpropagation learning methods are available, among them Levenberg-Marquardt algorithm was selected here because of its fastest convergence in the training of medium sized neural networks (Mathworks, 2007). This algorithm was developed to achieve a faster training speed without having to compute Hessian matrix and uses the update algorithm given by Eq. [2]:

$$\mathbf{x}_{k+1} = \mathbf{x}_k - [\mathbf{J}^T \mathbf{J} + \mu \mathbf{I}]^{-1} \mathbf{J}^T \mathbf{e} \quad [2]$$

where \mathbf{x}_k is the vector of weights and biases at the iteration of k ; \mathbf{J} is the Jacobian matrix, which contains first derivatives of the network errors with respect to weights and biases; \mathbf{J}^T is transpose matrix of \mathbf{J} ; \mathbf{e} is the vector of network errors; \mathbf{I} is the identity matrix; and μ is a scalar; μ decreases after each successful step and increases when an individual step increases the performance function and consequently, the performance function will always be reduced at each iteration of the algorithm (Mathworks, 2007).

The early stopping method was used in this study to prevent over-fitting (*i.e.* memorizing the available data by

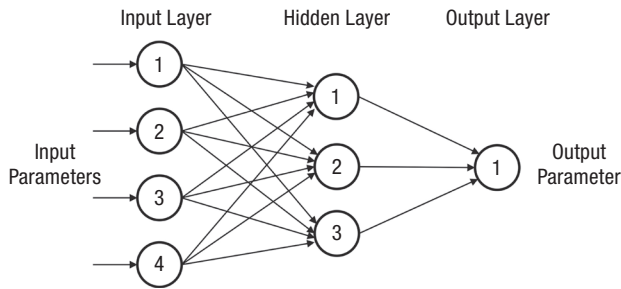


Figure 2. Scheme of multi-layer perceptron (MLP) neural network.

the network) and to achieve a good generalizing capability of the model. To perform this, the data were randomly divided into three subsets; one-half was used for training, one-quarter for validation and one-quarter for testing. The error, *i.e.* the difference between the measured target values and network results were calculated for each of the three subsets separately. During the early training iterations, the error on the validation subset normally decreases. However, when the network begins to over-fit the data, the validation subset error will start to rise. When this increase persists for a pre-defined number of iterations, the training is stopped and the weight values are kept.

The accuracy of dividing dataset was examined using the test subset. The errors on the test and validation subsets were compared to see if they showed a similar behavior. A significant difference between validation errors and test errors indicates an inappropriate division of the data.

The efficiency of network training increased by means of pre-processing and normalizing the network input and target values. Eq. [3] was used to normalize the data so that they fall in the range $[-1, 1]$:

$$x_{norm} = 2 \times \left(\frac{x_o - x_{min}}{x_{max} - x_{min}} \right) - 1 \quad [3]$$

where x_{norm} is normalized value; x_o is original value; x_{max} is maximum value; and x_{min} is minimum value.

Performance functions

The performance of the neural network models was evaluated by the root mean squared error (*RMSE*) as presented in Eq. [4]:

$$RMSE = \sqrt{\frac{1}{P} \sum_{i=1}^p [(PR_o)_i - (PR_s)_i]^2} \quad [4]$$

where the subscripts *o* and *s* represent the observed and simulated values of precipitation rates (*PR*) at each catch-can, respectively and *p* is the total number of events considered. The overall performance of trained networks can be judged with respect to coefficient of determination (R^2).

The Normalized Root Mean Square Error (*NRMSE*) was also calculated by dividing the *RMSE* value by the difference in value between the observed maximum and minimum precipitation rates as shown in Eq. [5]:

$$NRMSE = \frac{RMSE}{PR_{o(max)} - PR_{o(min)}} \quad [5]$$

Results

Selection of optimal ANN structure

A multi-layer perceptron with backpropagation training algorithm was used for simulation of single sprinkler distribution pattern. A tangent-sigmoid transfer function was selected between the input and hidden layers, and a linear transfer function selected between the hidden and output layer; because with sufficient neurons in the hidden layer this structure for a neural network is reported to have the ability to approximate any function (Mathworks, 2007).

Using the Neural Network Toolbox in MATLAB®, various networks with different configurations were defined in order to identify the optimal network for estimating the amount of water in each catch-can. All the designed neural networks contained three neurons in the input layer and one neuron in the output layer. For each distinct network, after post-processing, the *RMSE* and R^2 values for the training, validation and testing subsets were calculated.

Table 1 summarizes the results of the procedure for optimal network selection. The results showed that the neural networks containing one hidden layer were not able to estimate target values with sufficient accuracy ($R^2 < 0.861$ and $RMSE > 8.97$ mL for testing subset); hence, a network with two hidden layers was implemented. According to the evaluation results of various network structures, a network with two hidden layers, consisting of twenty neurons in the first hidden layer and six neurons in the second hidden layer, was determined as the optimal network, because any additional neurons in the hidden layer could not increase model accuracy.

Table 1. Summarized results for procedure of optimal network determining

Network structure	Training epochs	RMSE (mL)			R ²		
		Training	Validation	Testing	Training	Validation	Testing
3-5-1	116	10.68	10.65	10.77	0.816	0.810	0.809
3-6-1	83	10.45	10.43	10.78	0.820	0.829	0.810
3-7-1	12	13.12	13.35	13.13	0.724	0.704	0.718
3-8-1	33	12.12	13.59	12.24	0.758	0.711	0.751
3-9-1	254	9.49	9.80	9.52	0.854	0.854	0.837
3-10-1	161	9.30	9.50	8.97	0.860	0.858	0.861
3-5-5-1	64	11.93	11.40	11.58	0.772	0.783	0.775
3-6-5-1	42	7.24	7.44	7.19	0.914	0.913	0.913
3-7-5-1	53	8.22	8.40	8.04	0.891	0.885	0.891
3-8-5-1	60	7.18	7.09	6.94	0.915	0.922	0.919
3-9-5-1	88	8.27	8.92	8.03	0.888	0.869	0.896
3-10-5-1	58	8.32	8.35	8.09	0.889	0.881	0.892
3-11-5-1	161	6.57	7.19	7.63	0.929	0.914	0.909
3-12-5-1	84	6.68	7.48	6.69	0.927	0.913	0.923
3-13-5-1	64	6.90	7.05	7.64	0.921	0.920	0.909
3-14-5-1	22	13.05	13.12	12.81	0.726	0.710	0.725
3-15-5-1	94	7.00	7.86	7.01	0.919	0.904	0.918
3-20-5-1	36	7.07	7.55	6.46	0.919	0.906	0.930
3-5-6-1	62	7.14	6.99	7.57	0.918	0.919	0.906
3-10-6-1	39	7.05	6.74	7.64	0.918	0.925	0.910
3-11-6-1	120	6.66	6.76	7.36	0.928	0.924	0.911
3-12-6-1	235	6.96	6.91	7.35	0.922	0.920	0.912
3-15-6-1	36	8.06	7.67	9.03	0.895	0.902	0.866
3-20-6-1	144	6.46	6.81	6.69	0.931	0.925	0.929
3-10-10-1	72	6.89	7.76	6.93	0.921	0.902	0.925
3-15-15-1	56	7.09	7.52	7.26	0.916	0.910	0.917
3-20-20-1	84	7.07	7.34	7.45	0.920	0.908	0.907

As shown in Table 1, this structure for a neural network provides an $RMSE = 6.46, 6.81, 6.69$ mL and $R^2 = 0.931, 0.925, 0.929$ for training, validation and testing subsets, respectively. According to the t -test results, there was no significant difference at the probability level of 95% between the $RMSE$ and R^2 values for divided subsets. Also, the $RMSE$ and R^2 values for the testing subset (that were not used in the training of neural networks) indicated a good generalization ability of the selected structure.

Developing of ISSP

The selected structure of ANNs was implemented to develop a model named ISSP (Intelligent Simulator of Irrigation Pattern) as a MATLAB® m-file for the simulation of distorted distribution pattern from a R3000 sprinkler under experimental test conditions. This MATLAB m-file follows seven steps to simulate the

distribution pattern of a R3000 sprinkler and display the results as: 1) input data; containing wind speed (up to 8 m s^{-1}) and wind direction (0-359 degree); 2) generation of input matrix, involves calculation of R and γ for each catch-can; 3) normalizing the input matrix, the input matrix must be entered in the experimental database and normalized; 4) simulation of output values, normalized input matrix passes through the MLP neural network and produces normal values of collected volume of water at each point; 5) post-processing the output values, the network produces outputs in the range $[-1, 1]$; then these outputs must be converted back into the same unit that was used for the original targets; 6) removing abnormal values; in this step, negative and very small values (values < 0.5 mL) are converted to zero; 7) displaying the simulated distribution pattern as a contoured precipitation lines, colors or 3D maps; and 8) creating an Excel file that contains volume of collected water (mL) at each point (catch-can), *i.e.* $PR_{C(R,\gamma),V}$ values.

Simulation of distribution patterns using ISSP

In order to represent the ability of the ISSP model and to simulate the distortion pattern from of a single sprinkler caused by increasing wind speed, six different wind speeds from 1 to 6 m s⁻¹ with step of 1 m s⁻¹ and one direction (North-West) were selected. Fig. 3 illustrates distribution patterns resulted from ISSP model for these six conditions.

According to defined parameters in Fig. 4, the down-wind (r_{dw}), up-wind (r_{uw}) and cross-wind (r_{cw}) throw radii of the sprinkler at various wind speeds were presented in Fig. 5. Table 2 shows the range of wetted area at x and y directions, the coordinates for the centre of the wetted area and the resultant shifts in wetted area due to wind (*i.e.* distance of sprinkler position to the center of the wetted area). Fig. 6 shows amount of wetted area drifting *vs.* wind speed.

Table 2. Characteristics of wetted area ranges and its drifting due to various wind speeds

Wind speed (m s ⁻¹)	X range [x ₁ , x ₂]	Y range [y ₁ , y ₂]	Center (x _c , y _c)	Drift (m) ¹
1	[-7.75, 8.75]	[-8.70, 8.13]	(0.50, -0.29)	0.52
2	[-7.50, 8.80]	[-8.75, 7.92]	(0.65, -0.42)	0.77
3	[-7.08, 9.38]	[-9.17, 7.50]	(1.15, -0.83)	1.42
4	[-6.25, 9.75]	[-9.40, 7.00]	(1.75, -1.20)	2.12
5	[-6.20, 10.00]	[-10.00, 7.00]	(1.90, -1.50)	2.42
6	[-5.00, 10.00]	[-10.80, 6.80]	(2.50, -2.00)	3.20

¹ Distance of sprinkler position to the center of the wetted area.

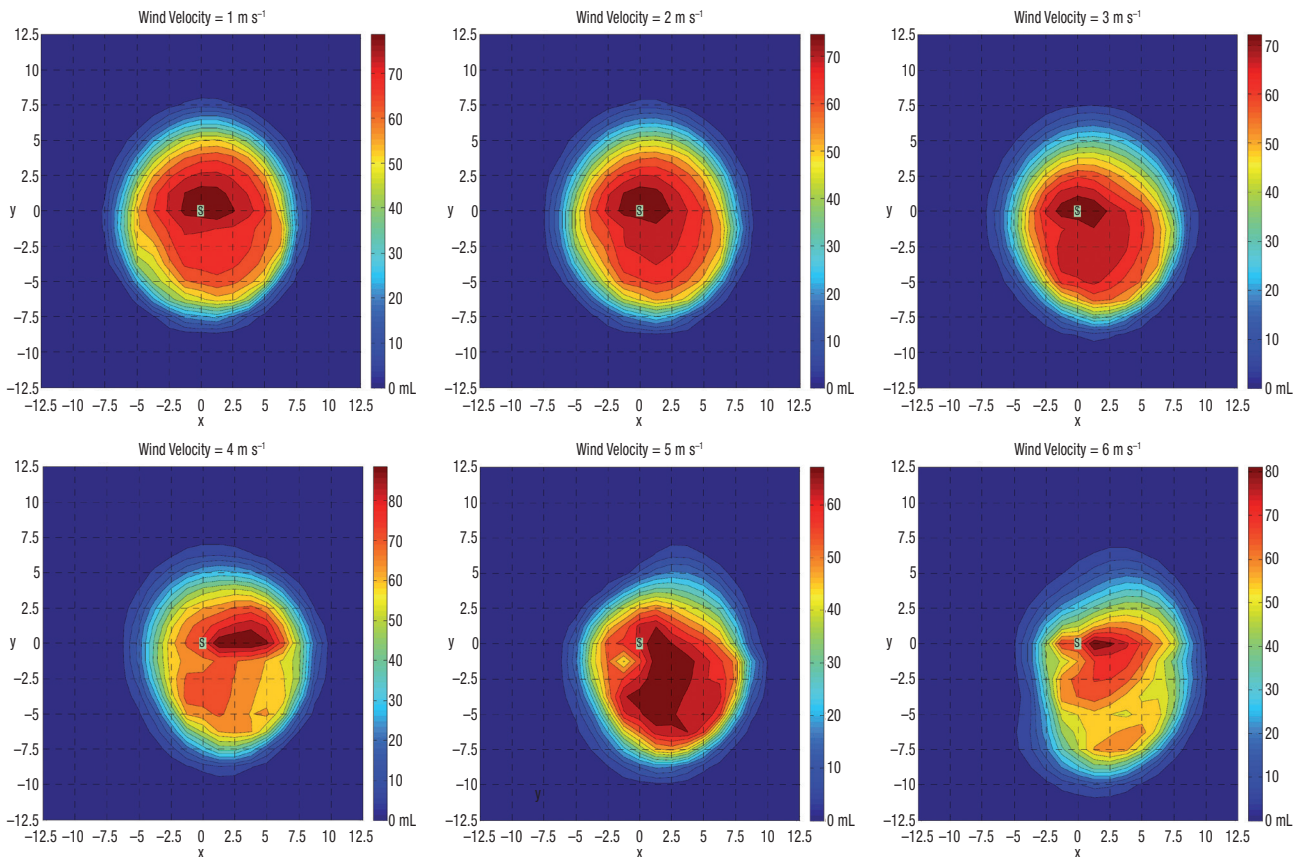


Figure 3. Simulation of distribution pattern distortion process by ISSP (“S” indicates sprinkler position). Wind direction = 135 degrees.

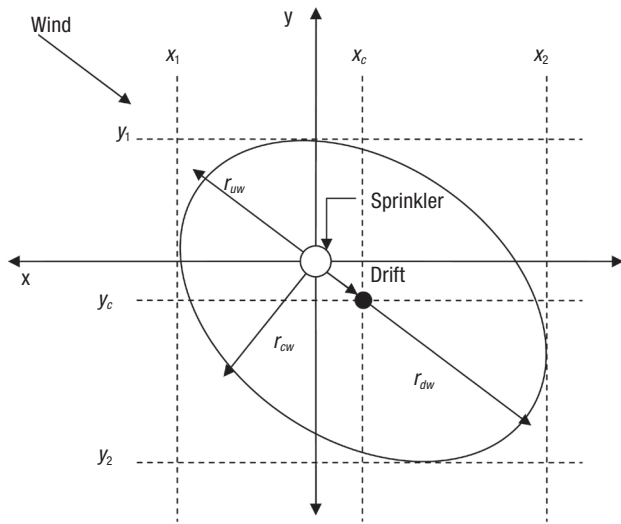


Figure 4. Schematic view of throw radii from sprinkler and the shift of the wetted area according to the wind direction

Moreover, for the sake of comparison between simulated and observed distribution patterns three different conditions were considered a) a wind speed of 0.63 m s^{-1} and direction of 11 degrees, b) a wind speed of 2.65 m s^{-1} and direction of 176 degrees and c) wind speed of 4.60 m s^{-1} and direction of 158 degrees. These conditions selected from an experimental dataset to represent low, medium and high wind speeds. Fig. 7 illustrates the simulated and observed distribution patterns for each of these three conditions.

Fig. 8 represents the scatter plots for simulated versus observed $PR_{C(R,y),V}$ values for these three conditions, from which it can be observed that there were good correlations between simulated and observed values for precipitation rate. Table 3 summarizes the

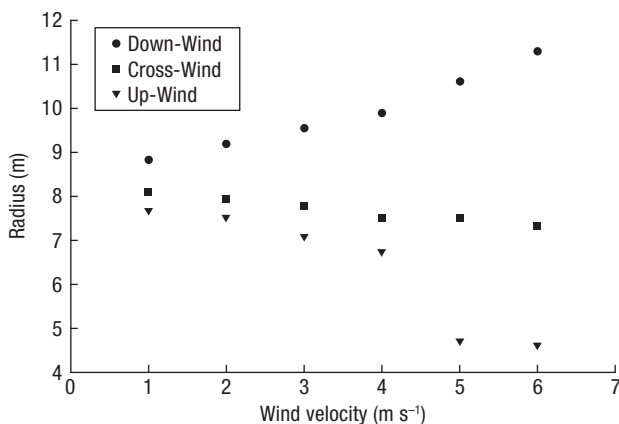


Figure 5. Down-wind (r_{dw}), up-wind (r_{uw}) and cross-wind (r_{cw}) throw radii of sprinkler at various wind velocities.

evaluation results for simulated distribution patterns (i.e. maximum precipitation depths, cumulative volumes of water collected in catch-cans and absolute difference, $RMSE$, $NRMSE$ and R^2 between simulated and observed values).

Discussion

Comparison of simulated and observed distribution patterns

According to the observed and simulated distribution patterns (Fig. 7) it is recognized that the simulated distribution patterns have smoother shapes since these patterns do not have obvious peak and dip points and the amount of water collected in each catch-can differs gradually from one location to another.

Fig. 8 and Table 3 show that in all three conditions, the R^2 values are higher than 0.935 and the differences between them are very small; hence there is good correspondence between the model results and observed values. While there are some underestimations in the values for maximum precipitation depth, these differences decrease as the wind speed increases. According to Table 3, the cumulative volumes of collected water for both simulated and observed values decrease as the wind speed increases. This could be due to the fact that a proportion of emitted drops drifts out of the catch-can network due to wind and the ANN based model has an ability to learn this phenomenon through the process of training with an experimental dataset. In addition, according to the values of $NRMSE$, R^2 and absolute difference between calculated and observed data, the

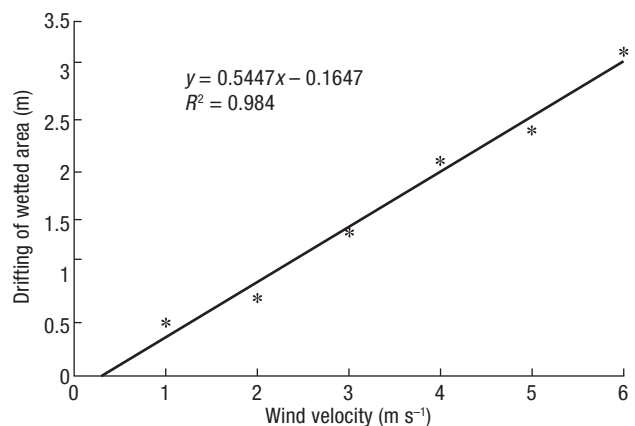


Figure 6. Amount of wetted area drifting versus wind speed.

Table 3. Results of sample simulated and observed distribution patterns evaluations

	Maximum PR (mL)			Cumulative PR (mL)			RMSE (mL)	NRMSE (%)	R ²
	Obs ¹	Sim ²	Dif ³	Obs ¹	Sim ²	Dif ³			
a	90	82.4	7.6	6,373	6,316	57	6.16	6.84	0.945
b	85	80.7	4.3	5,406	5,726	320	5.85	6.88	0.941
c	82	78.5	3.5	5,054	5,524	470	5.72	6.97	0.935

¹ Observed value. ² Simulated value. ³ Absolute difference between observed and simulated values.

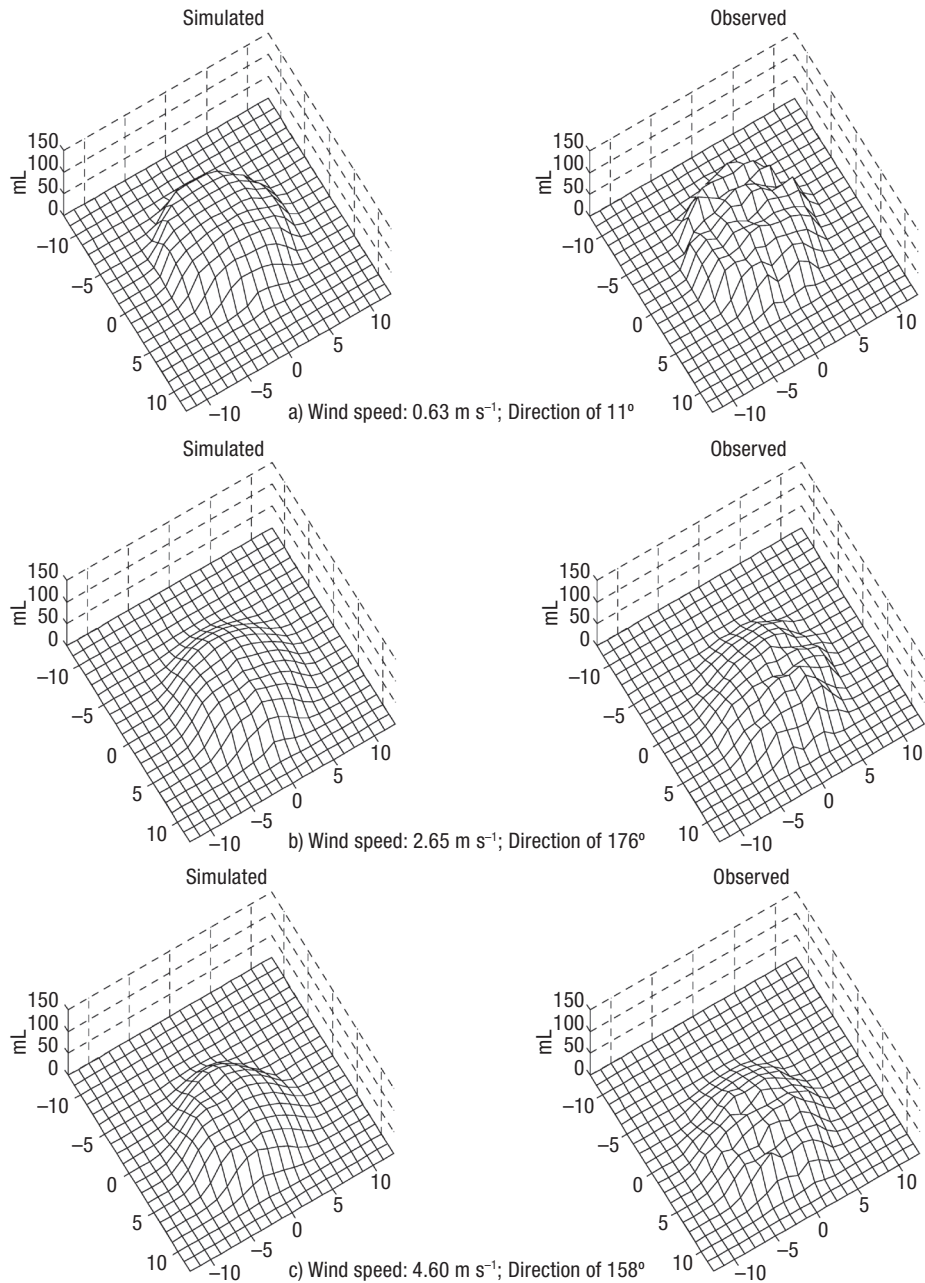


Figure 7. Comparison of simulated and observed distribution patterns for three conditions of wind speed and direction.

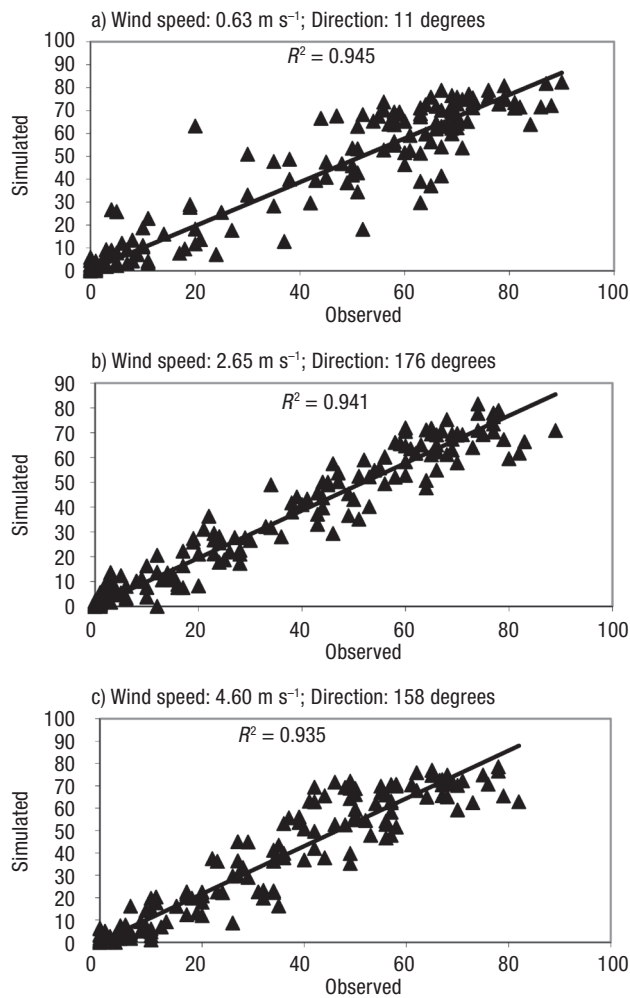


Figure 8. Simulated versus observed $PR_{C(R,T),V}$ values for three conditions of wind speed and direction.

model error slightly increases as wind speed increases, but the model results still remain robust.

Assessing the shapes of simulated wetted areas

The shapes of the simulated wetted areas (Fig. 3) have been evaluated for range shortening and shifting of the wetted area due to wind. According to Fig. 3, Fig. 5 and Table 2 the following important points can be highlighted: 1) the up-wind and cross-wind throw radii decreases as wind speed increases; 2) the down-wind throw radii increased as wind speed increased; 3) the ISSP model successfully simulated the shift in wetted area due to wind; as shown in Fig. 3 and Table 2, where the wetted area of a single sprinkler shifts to

East-South due to the North-West direction of the wind; the amount of shifting increases as wind speed increases; and 4) In Fig. 6 there is a linear relationship between the shift in wetted area and wind speed.

Although in developing the ISSP no pre-assumptions were considered for the modification of distribution pattern due to wind (in contrast to semi-empirical models) all the results presented here are in accordance with the hypothesis used for the development of semi-empirical models (Richards & Weatherhead, 1993; Le Gat & Molle, 2000; Granier *et al.*, 2003).

The ISSP, as a first step in developing an intelligent model for simulating a single sprinkler distribution pattern, is not a general and comprehensive model, but the results obtained from model evaluation confirm its accuracy and robustness of ANNs for the simulation of a single sprinkler distribution pattern under real field conditions. The model presented can reliably simulate the water distribution patterns for different windy conditions and does not produce any abnormal and/or irregular shaped distribution patterns.

It seems that the next step in the field for using ANNs for simulation of a single sprinkler distribution pattern would be to develop a general and comprehensive model. Such a general model would be able to simulate any single sprinkler distribution pattern on the basis of a preliminary distribution pattern measured in laboratory condition and also wind specifications.

Acknowledgement

This research was supported by the Department of Research and Technology, University of Tabriz. The use of certain products in this study does not imply any endorsement of them. The authors thank Dr. Jerry Knox (Cranfield University, UK) by the revision of the manuscript.

References

- Anonymous, 2008. Water application solutions for centre pivot irrigation. Nelson Irrigation Co. Available online in http://www.nelsonirrigation.com/data/products/Pivot_pocketguide4.pdf [6 September 2011].
- ASAE, 1985. Standard S398.1. Procedure for sprinkler testing and performance reporting. ASAE standards, ASABE, St Joseph, MI, USA.

- Basheer IA, Hajmeer M, 2000. Artificial neural networks: fundamentals, computing, design, and application. *J Microbiol Meth* 43: 3-31.
- Carrion P, Tarjuelo JM, Montero J, 2001. SIRIAS: a simulation model for sprinkler irrigation: I. Description of model. *Irrig Sci* 20: 73-84.
- Ciğizoğlu HK, 2002. Suspended sediment estimation for rivers using artificial neural networks and sediment rating curves. *Turk J Eng Environ Sci* 26: 27-36.
- De Wrachien D, Lorenzini G, 2006. Modelling jet flow and losses in sprinkler irrigation: Overview and perspective of a new approach. *Biosyst Eng* 94(2): 297-309.
- Dechmi F, Playan E, Cavero J, Martinez-Cob A, Faci JM, 2004. Coupled crop and solid set sprinkler simulation model: I. Model development. *J Irrig Drain Eng* 130(6): 499-510.
- Fernando DAK, Jayawardana AW, 1998. Runoff forecasting using RBF networks with OLS algorithm. *J Hydrol Eng* 3(3): 203-209.
- Fukui Y, Nakanishi K, Okamura S, 1980. Computer evaluation of sprinkler irrigation uniformity. *Irrig Sci* 2: 23-32.
- Granier J, Molle B, Deumier JM, 2003. IRRIPARC-Part 1: Modeling spatial water distribution under a sprinkler in windy conditions – Utilization of the IRRIPARC methodology in 3 regions. *Proc ICID Int Workshop on Improved Irrigation Technologies and Methods: Research, development and testing*. Montpellier, France, pp: 14-19.
- Han S, Evans RG, Kroeger MW, 1994. Sprinkler distribution patterns in windy conditions. *T ASAE* 37(5): 1481-1489.
- Haykin S, 1999. *Neural networks: A comprehensive foundation*. Prentice-Hall Inc, Engelwood Cliffs NJ, USA.
- Heermann DF, Duke HR, Serafim AM, Dawson LJ, 1992. Distribution function to represent center pivot water distribution. *T ASAE* 35(5): 1465-1472.
- Hinnell AC, Lazarovitch N, Furman A, Poulton M, Warrick AW, 2010. Neuro-Drip: estimation of subsurface wetting patterns for drip irrigation using neural networks. *Irrig Sci* 28 (6): 535-544.
- Hsu K, Gupta HV, Sorooshian S, 1995. Artificial neural network modeling of the rainfall-runoff process. *Water Resour Res* 31(10): 2517-2530.
- ISO, 1995. ISO Standard 8026. *Agricultural irrigation equipment-Sprayers-General requirements and test methods*. ISO, Lethbridge, Alberta, Canada.
- Jain SK, Singh VP, Van Genuchten MTh, 2004. Analysis of soil water retention data using artificial neural networks. *J Hydrol Eng* 9(5): 415-420.
- Karmeli D, 1978. Estimating sprinkler distribution patterns using linear regression. *T ASAE* 21: 682-686.
- Karul C, Soyupak S, Cilesiz AF, Akbay N, German E, 2000. Case studies on the neural networks in eutrophication modeling. *Ecol Model* 134: 145-152.
- Keller J, Bliesner RD, 1990. *Sprinkle and trickle irrigation*. AVI Book, Van Nostrand Reinhold. New York.
- Khoob AR, 2007. Comparative study of Hargreaves's and artificial neural network's methodologies in estimating reference evapotranspiration in a semiarid environment. *Irrig Sci* 26(3): 253-259.
- Kincaid DC, 2005. Application rates from center pivot irrigation with current sprinkler types. *Appl Eng Agric* 21(4): 605-610.
- Lazarovitch N, Poulton M, Furman A, Warrick AW, 2009. Water distribution under trickle irrigation predicted using artificial neural networks. *J Eng Math* 64: 207-218.
- Le Gat Y, Molle B, 2000. Model of water application under pivot sprinkler: I. Theoretical grounds. *J Irrig Drain Eng* 126(6): 343-347.
- Lorenzini G, 2004. Simplified modelling of sprinkler droplet dynamics. *Biosyst Eng* 87(1): 1-11.
- Maier HR, Dandy GC, 2000. Neural networks for the prediction and forecasting of water resources variables: a review of modeling issues and applications. *Environ Model Softw* 15: 101-124.
- Mathworks Inc., 2007. *Neural network toolbox 5 user's guide*, 9th printing, vers 5. The Mathworks Inc. Natick, MA, USA.
- Molle B, Le Gat Y, 2000. Model of water application under pivot sprinkler: II. Calibration and results. *J Irrig Drain Eng* 126(6): 348-354.
- Montero J, Tarjuelo JM, Carrion P, 2001. SIRIAS: a simulation model for sprinkler irrigation: II. Calibration and validation of the model. *Irrig Sci* 20: 85-98.
- Ozkan C, Kisi O, Akay B, 2011. Neural networks with artificial bee colony algorithm for modeling daily reference evapotranspiration. *Irrig Sci* 29(6): 431-441.
- Playan E, Zapata N, Faci JM, Tolosa D, Lacueva JL, Pelegrin J, Salvador R, Sanchez I, Lafita A, 2006. Assessing sprinkler irrigation uniformity using a ballistic simulation model. *Agr Water Manage* 8(4): 89-100.
- Richards PJ, Weatherhead EK, 1993. Prediction of raingun application patterns in windy conditions. *J Agric Eng Res* 54(4): 281-291.
- Schleiter IM, Borchardt D, Wagner R, Dapper T, Schmidt KD, Schmidt HH, Werner H, 1999. Modeling water quality bioindication and population dynamics in lotic ecosystems using neural networks. *Ecol Model* 120: 271-286.
- Schmitz GH, Schutze N, Petersohn U, 2002. New strategy for optimizing water application under trickle irrigation. *J Irrig Drain Eng* 128(5): 287-297.
- Seginer I, Nir D, Von Bernuth ED, 1991a. Simulation of wind-distorted sprinkler patterns. *J Irrig Drain Eng* 117(2): 285-306.
- Seginer I, Kantz D, Nir D, 1991b. The distortion by wind of the distribution patterns of single sprinklers. *Agric Water Manage* 19(4): 341-359.
- Shrestha RR, Theobald S, Nestmann F, 2005. Simulation of flood flow in a river system using artificial neural networks. *Hydrol Earth Syst Sci* 9(4): 313-321.

- Solomon K, Bezdek JC, 1980. Characterizing sprinkler distribution patterns with a clustering algorithm. *T ASAE* 23(4): 899-902.
- Vories ED, Von Bernuth ED, Mickelson RH, 1987. Simulating sprinkler performance in wind. *J Irrig Drain Eng* 113(1): 119-130.
- Yan HJ, Bai G, He JQ, Li YL, 2010. Model of droplet dynamics and evaporation for sprinkler irrigation. *Biosys Eng* 106: 440-447.
- Yang CC, Prasher SO, Lacroix R, Sreekanth SRI, Patni NK, Masse L, 1997. Artificial neural network model for subsurface-drained farmlands. *J Irrig Drain Eng* 123(4): 285-292.